Structural, dielectric and piezoelectric properties of the ferroelectric PZT-BT ceramic compounds

C. MICLEA[a,*], C. F. MICLEA[a], L. AMARANDE[a], C. T. MICLEA[b,c], M. CIOANGHER[a]
[a]*National Institute for Materials Physics, Str. Atomistilor 405A, Magurele, Romania*
[b]*University of Bucharest, Faculty of Physics, Str. Atomistilor 405, Magurele, Romania*
[c]*Hyperion University, Faculty of Physics, Str. Calarasi 169, Bucharest, Romania*

Ceramic compounds of ferroelectric lead zirconate titanate (PZT) and ferroelectric barium titanate (BT) were prepared from nanopowders corresponding to the formula (1-*x*)PZT·*x*BT with x = 0; 0.1; 0.2 … 0.9; 1. The samples were investigated by X-ray diffraction and electron microscopy and the piezoelectric properties were determined by means of an impedance analyzer. The sintering process is complex since samples densify at different temperatures depending on the composition resulting in different morphostructures. Accordingly, the piezoelectric properties show unusual behavior discussed in terms of different grain size and composition. A remarkably high enhancement of the relative dielectric constant, ε_r coupled with maxima in both, piezoelectric charge constant d_{33} and the piezoelectric voltage constant g_{33}, is observed for x = 0.4 while the values of the coupling coefficient kp are still high similar to those of pure PZT.

(Received June 25, 2018; accepted October 10, 2018)

Keywords: PZT, BT, Mixed structure, Dielectric properties, Piezoelectric properties, Grain size

1. Introduction

Multiferroic materials are those materials that possess two or three ferroic properties such as ferroelectricity, ferroelasticity and ferromagnetism [1-4]. Though the research into ferroic materials took off during the second half of the last century when the linear magnetoelectric effect was predicted in chromium oxide [5], it was only during the last years that multiferroics have attracted tremendous attention and a revival of the field was observed [3, 6-10] mainly due to the exciting application potential in multiple controlled devices [2, 11-14] such as modulation of amplitudes, polarization and phases of optical devices, data storage and switching, optical diodes, spin wave generation, amplification and frequency conversion [3]. Multiferroic materials may exist either in single phase form or in two phase systems. While the former is limited in number, the latter one, which can be achieved in the form of ceramic compounds or laminates, may be found in a large variety of combinations. In the two phase systems the most used ferroic substances are barium titanate and lead titanate zirconate combined with different magnetic materials [15-21].

In the present investigation we have prepared a number of ferroic compositions made from barium titanate (BT) and lead titanate zirconate (PZT), known as the most representative members of the family of ferroelectric materials during the last decades due to their exceptionally properties [22-24].

Barium titanate is a typical perovskite material with the formula $BaTiO_3$ and its main piezoelectric parameters as follows: electromechanical coupling factor, k_p = 0.35-0.4; dielectric constant, ε_r = 1000÷3000; charge constant, d_{33} around 200 pC/N; voltage constant, g_{33} around 10^{-2} Vm/N [25-27]. Piezoelectric barium titanate was the first ceramic material ever developed to be used as a transducer but now it is almost exclusively used as high dielectric constant capacitor [20, 28]. Between room temperature and about 130 °C it has a tetragonal structure and its basic ions (Ba and Ti) can be partially replaced in order to enhance some special properties.

On the other hand the ferroic material lead titanate-zirconate known as PZT material has better piezoelectric parameters than BT, namely a much higher electromechanical coupling factor, k_p = 0.6-0.7; a dielectric constant, ε_r around 1500, a charge constant, d_{33} of 300-500 pC/N and a voltage constant, g_{33} of $25 \cdot 10^{-3}$ Vm/N. Other new piezoceramic materials with properties superior to those of the PZT class have not been yet discovered. Structurally, the PZT type materials crystallize in the perovskite form and practically all ions of the basic composition can be partially replaced by isovalent and/or isovalent ions in order to obtain a rather endless number of new materials with different parameters.

In spite of their virtues as individual materials, the PZT and BT were not mixed together to form new materials with new properties except in the last few years when the interest for such mixed material arose. The present authors made first trials in this direction some years ago [29]. The subject was revived by a group of Thailandese researchers [30-35]. They made solid solutions of PZT and BT on the whole compositional interval and studied some of the dielectric and ferroelectric properties of such composition.

The objective of the present investigation is to prepare mixtures of nanopowders of piezoelectric compositions from a soft type piezoceramic material situated within the morphotropic phase boundary and the classic piezoelectric barium titanate within the whole interval from pure PZT to pure BT and to investigate their main morphostructural and piezoelectric properties.

2. Experimental

2.1. Powders preparation

There are several ways to synthesize both PZT and BT materials. Among them the mixed oxides technology followed by solid state reaction proved to be the easiest and the cheapest one. But it has a drawback, namely both chemical and morphostructural homogeneity are rather poor. In addition, it produces micron scale powders. Chemical and mechanochemical activation routes solved, to a great extent, these problems but they are laborious and rather expensive. Nanometric powders are required for a better and faster chemical reaction at high temperature. Therefore, in order to produce nanoscale powders we made a compromise between the conventional mixing oxide route and mechanical activation, consisting in that the initial powders were prepared by the mixing oxide route followed by solid state reaction and then the reacted powders were grinded in an energy planetary ball mill for a longer time to produce the desired nanopowders.

2.1.1. The ferroic PZT powder

The composition chosen for the experiment was the following: $Pb_{0.98}Sr_{0.02}Zr_{0.50}Ti_{0.45}Nb_{0.05}O_3$. Both Sr and Nb were added in order to imprint the composition a soft ferroelectric character [36] and to keep it within the morphotropic phase boundary. High purity oxides (over 99.2 %) from Merck, Fluka and Riedel de Haen were used as raw materials. The stoichiometric amounts of oxides were mixed together in ethanol for 4 hours in a planetary ball mill, then the slurry was dried and manually crushed and sieved. The resulted powder was calcined in dense alumina crucibles, in a chamber furnace at 900 ^oC for 3 hours. The white yellow agglomerated powder resulted after calcining was again crushed and sieved and then subjected to a prolonged milling for 24 hours in a high energy planetary ball mill Retsch PM 400. This final milling was carried out in agate jars, with agate balls at a ball/powder ratio of 4/1. The rotation speed of the mean wheel of the mill was set at 350 rot $\cdot min^{-1}$ with a ratio for the jars of 1/2. The morphostructure of the milled powder was checked by X-ray diffraction and SEM microscopy.

2.1.2. The ferroic BT powder

The BT powder, corresponding to the formula $BaTiO_3$, was synthesized from pure barium carbonate $BaCO_3$ and titanium dioxide TiO_2 from Merck having purities of 99.95 and 99.97 % respectively. Stoichiometric amounts of each raw material were mixed for 4 hours in the planetary ball mill with methanol as milling medium. The slurry was dried, crushed and calcined at 1100 ^oC for 3 hours in alumina crucibles, in a chamber furnace. The white powder resulted after calcining was now milled for 24 hours in the same high energy planetary ball mill and in similar conditions as the PZT. Similar analysis was undertaken for this nanometric powder as well.

2.1.3. The ferroic PZT-BT mixtures

The ferroic PZT-BT mixed powder samples were processed to correspond to a generic formula of this type: $(1-x)PZT \cdot xBT$ with $x = 0; 0.1; 0.2 \ldots\ldots 0.9; 1$. The mixing proportions were made by weight in batches of 10 g in order to allow for easier further calculations. Thus, for example, for the composition with $x = 0.4$, we have mixed 4 g of BT with 6 g of PZT, and so on. The stoichiometric amounts of each nanopowder were mixed for 4 hours in the planetary ball mill, in methanol, in order to make the mixture as homogeneous as possible. The dried mixed powders were moistened with about 5 % wt. distilled water by spraying and then uniaxially pressed in a cylindrical steel die at a pressure of about 50 MPa. The pressed samples were next sintered on platinum closed boats at temperatures between 1100-1400 ^oC for 5 hours.

Density (Archimede method), X-ray diffraction (Siemens Kristalloflex IV with CuKα radiation) and SEM images (electron microscope HITACHI, S-2600N model) were carried out on sintered disc shaped samples. The samples for the piezoelectric properties measurements were prepared by mechanically polishing the sintered samples into disks of 10 mm diameter and 1 mm thickness with plan parallel faces. Silver electrodes were painted and fired at 610 ^oC for 10 minutes. Subsequently, the samples, immersed in a silicon oil bath at 100^oC, were poled under an electric field of 3 kV/mm applied on the electrodes for 5 minutes. The samples were then cooled down to room temperature while the field was kept constant. Piezoelectric properties were determined by means of an AGILENT 4294A impedance phase/gain analyzer 24 hours after poling.

3. Results and discussions

3.1. Structural properties

Figs. *1 (a)* and *(b)* and *2 (a)* and *(b)* illustrate the X-ray patterns and the morphology of the PZT and BT nanopowders respectively after calcining and milling for 24 hours in the high energy Retsch planetary ball mill. The X- ray patterns for both powders correspond to the perovskite structure with no secondary phases.

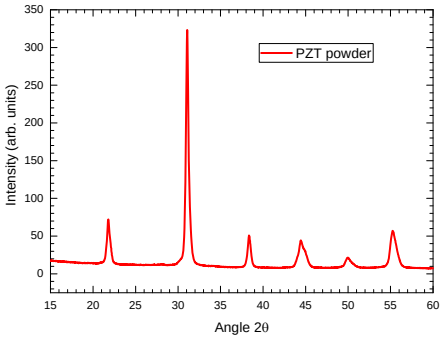

(a)

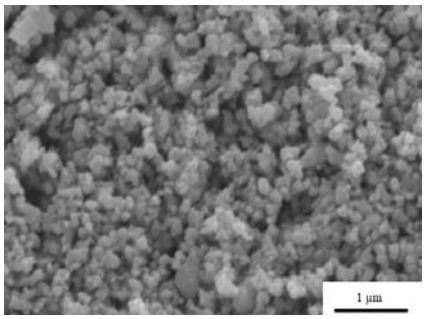

(b)

Fig. 1. (a). X-Ray patterns of PZT powder, after calcining and milling for 24 hours; (b). The morphostructure of the calcined PZT powder after milling. The average grain size is about 250 nm

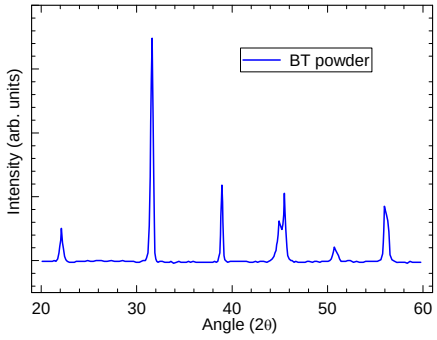

(a)

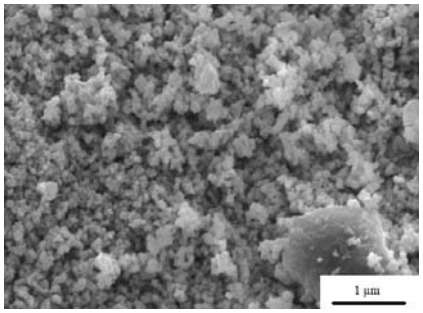

(b)

Fig. 2. (a). X-Ray patterns of BT powder, after calcining and milling for 24 hours; (b). The morphostructure of the calcined BT powder after milling. The average grain size is about 213 nm

The morphostructures shown in the SEM images of Figs. 1 b and 2 b look extremely similar for both powders. The average grain size was estimated to be about 250 nm for PZT and 213 nm for BT. These differences could be explained by the different mechanical properties of the two materials. For instance the compressive tensile strength for PZT is greater than 600 MPa while for BT it is around 50 MPa [38] and the hardness for PZT is about 6 Mohs while for BT is around 5 Mohs. Due to this facts, during the milling process, the BT particles break easier than the PZT ones and leading to eventually different grain sizes, despite the identical milling conditions.

The X-ray diagrams of the mixed and sintered samples of PZT and BT are shown in Fig. 3 for several compositions. One can see that there are no noticeable differences between the X-ray patterns of all these compositions. All of them show only the perovskite phase regardless of the ratio between PZT and BT. This is quite normal since both material have the same structure and similar elementary cells with nearly the same tetragonal distortion (for PZT $c/a \approx 1.02$ and for BT $c/a \approx 1.01$). A slight difference between them appears for compositions richer in PZT where the rhombohedral (200) peak appears and become important suggesting that these compositions are within the morphotropic phase boundary. It is also an indication that the microscopic homogeneity is not perfect and some compositional fluctuation at the particle level does exist.

The sintering process of the two different mixed powders is more complex than the one observed in the case of one single powder, because the optimum sintering temperature is significantly different for each separate compounds: lower for PZT of only about 1200 ^{o}C and higher for BT of about 1400 ^{o}C [38, 39].

Any polycrystalline compact sinters by the diffusion transport of matter which takes place via two main mechanisms, surface diffusion and volume diffusion respectively. These mechanisms lead to a better densification of ceramics. In the initial stage of sintering the inter particle necks grow rapidly by diffusion [40].

As the surface of the particles is not smooth, since it contains many structural defects like ledges, kinks, vacancies, dislocation, the surface diffusion involves motion of atoms between these sites, thermally activated, which means that temperature significantly influences the surface diffusion process. On the other hand, the volume diffusion, or lattice diffusion, takes place by the movement of point defects among which the vacancies play the most important role. In both mechanisms the matter transport from the site of the particles through the necks formed between them and further into the other particles, gives rise eventually, upon increasing sintering time and temperature, to crystallites of larger dimensions.

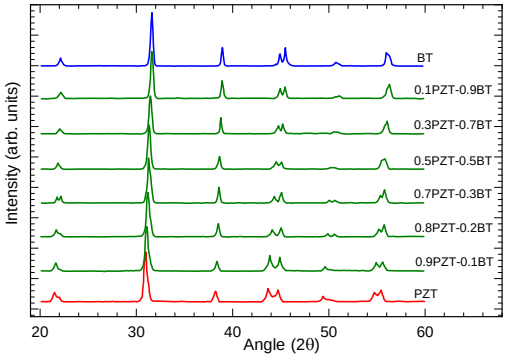

Fig. 3. X-Ray patterns of sintered mixed samples of PZT and BT for some compositions. Only perovskite phase is evidenced and no other foreign phase was detected

These processes in which coalescence of neighboring grains by which the density increases [41] are well illustrated in the SEM image of Fig. 4 for the composition with $x = 0.6$ and sintered at 1350 ^{o}C where one can see about 5 particles of BT surrounding in the middle a particle of PZT which is practically "swallowed" by diffusion. In the upper right side one can also see how two BT particles formed a large neck and finally they will grow unite into a single larger particle if the sintering time or/and the temperature increase.

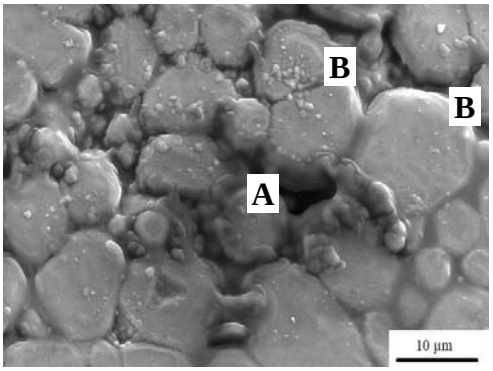

Fig. 4. SEM micrograph of the composition with x=0.6 sintered at 1350 ^{o}C. One can see a PZT particle (A) surrounded by about 5 particles of BT being practically "melted" and incorporated into BT matrix. A well-defined neck between BT particle (A) can be observed (BB)

Assuming the ideal model of spheres [40] one can easily estimate for each mixing proportion, the number of particles of one specie surrounding one particle from the other species. Knowing the average diameter of each powder grain and their densities one can calculate the average mass of one particle and the corresponding number of particles per gram. By determing the mass ratio between the two species one can easily estimate the distribution of particles of each type for a certain concentration of the composition. The results of the calculation are shown in Table 1 in which for each mixed proportion of BT and PZT is indicated how many particles of BT surround one single particle of PZT.

Table 1

x from (1-x)PZTxBT	0	0.1	0.2	0.3	0.4
No. of BT particles surrounding one PZT particle	0	0.283	0.636	1.092	1.698

x from (1-x)PZTxBT	0.5	0.6	0.7	0.8	0.9
No. of BT particles surrounding one PZT particle	2.547	3.821	5.945	10.189	22.93

Thus for the situation presented in Fig. 4, there are about 5 BT particles surrounding 1 PZT particle, which corresponds in Table 1 to compositions with x = 0.6 and x = 0.7. This confirms the model since the picture in Fig. 4 was indeed taken for the composition with x = 0.6.

Fig. 5 (a) shows the dependence of the maximum density, ρ as a function of the composition concentration x and the Fig. 5 (b) displays the optimum sintering temperature, T_{os} for each composition when the density was maximum. These values were determined from the plots showing the behavior of the density with sintering temperature for all concentration range investigated.

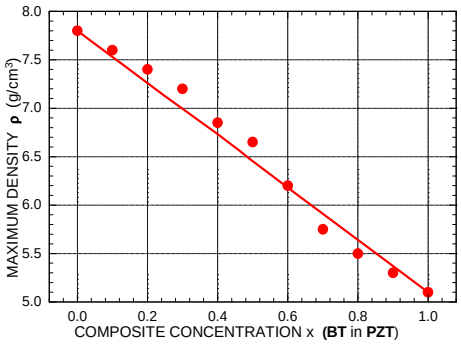

(a)

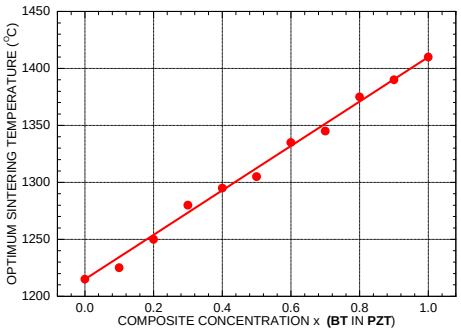

(b)

Fig. 5. (a). The dependence of the maximum density on composition concentration x for mixed PZT and BT samples; (b). The dependence of the optimum sintering temperature on the composition concentration x for mixed PZT and BT samples

As can be seen the dependences for both ρ and T_{os} are roughly linear, with ρ reduced and T_{os} enhanced upon increasing the concentration x. The existing small deviations can be ascribed to slight structural inhomogeneities of the samples.

Fig. 6 (a), (b) and (c) illustrate the mechanical fracture behavior of ceramic compounds with different concentration. Thus fig. 6a corresponds to x = 0.8 being characteristic to compositions richer in BT. One can see that the fracture is mainly trans-granular while Fig. 6 c corresponding to the composition with x = 0.1, richer in PZT, is mainly inter-granular. From the compositions situated within the middle of the compositional interval, the fracture behavior is both trans- and inter- granular as illustrated in Fig. 6 b. Such a behavior could be explained by the following possible mechanism.

The compositions rich in PZT, corresponding to lower x, contain a small number of BT particles resulting in the decrease of sintering temperature. Probably the mixture is mainly mechanical and solid solutions between PZT and BT form very hardly.

In this case the fracture is mainly inter-granular. As the sintering temperature increases and the compositions of BT and PZT equilibrate, the PZT phase starts to transform into a liquid phase that helps densification and it is "swallowed" by the BT phase, and so the fracture is both trans- and inter- granular as can be seen in Fig. 6 (b).

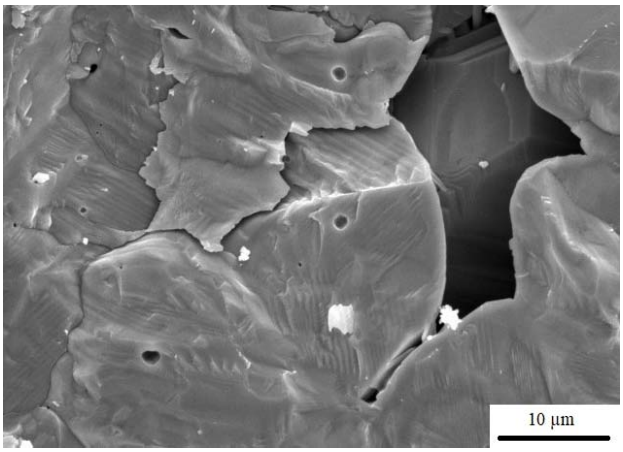

(a)

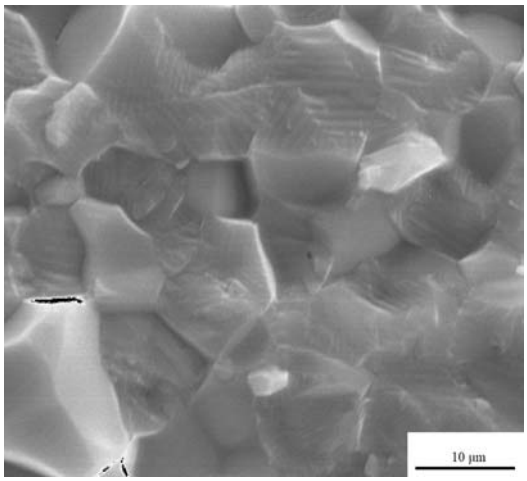

(b)

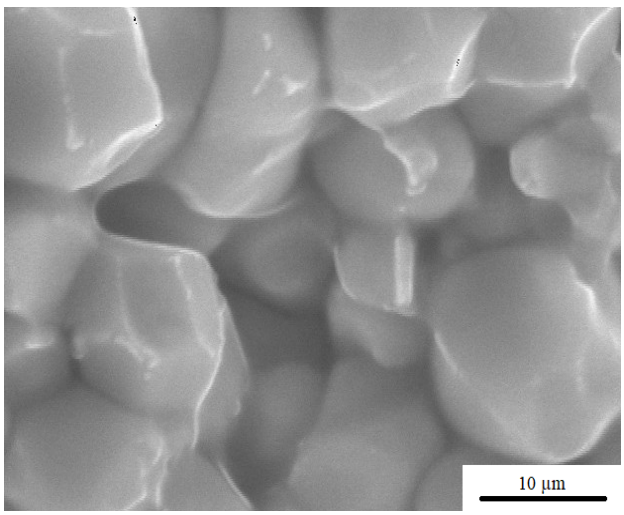

(c)

Fig. 6. (a). SEM fracture micrograph of sintered sample with x=0.8 sintered at 1400 °C; (b). SEM fracture micrograph of sintered sample with x=0.5 sintered at 1300 °C; (c). SEM fracture micrograph of sintered sample with x=0.1 sintered at 1200 °C

Toward the end of the interval where the BT phase become predominant and PZT phase is small, it becomes liquid, since the sintering temperature is higher and the fracture is entirely inter-granular (Fig. 6 (c)).

3.2. Dielectric and piezoelectric properties

The permittivity is an important parameter for ferroic ceramic compounds regarding the material selection for applications because materials with higher permittivity require lower electric fields compared to those with lower permittivity. This improves the electrical efficiency. The relative permittivity ε_r, was calculated by the capacitance, C, measurements making use of the basic equation

$$C = \varepsilon_r \varepsilon_0 A/h \tag{1}$$

where A is the active sample area, h is the sample thickness and ε_0 the permittivity of free space.

Fig. 7 shows the behavior of the relative dielectric constant ε_r as a function of compositions. It is interesting to note that both end compositions show nearly the same values for ε_r of around 1500, while the middle compositions exhibit a rather sharp maximum with the highest value of 7000 for the compositions with 0.6 PZT·0.4 BT and 0.5 PZT·0.5 BT. This behavior could be associated with the crystallite size. At both ends there is a non-uniform distribution of the crystallites due to the inhomogeneity of the compositions involved. At the middle of the compositional range the distribution is more uniform and probably the crystallite size is at an optimum for the high dielectric constant. It is known that the dielectric constant is strongly dependent on the grain size [42-44]. Coarse grain ceramics show lower dielectric constant than fine grain ones [45]. But there is an optimum grain size where the dielectric constant shows a maximum value [46].

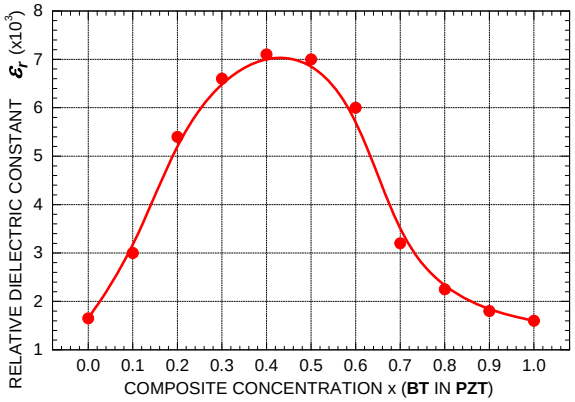

Fig. 7. The dependence of the relative dielectric constant on concentration x for sintered mixed PZT and BT samples

Fig. 8 shows the dependence of the planar coupling coefficient k_p on composition. For pure PZT the k_p is 0.59 and upon the introduction of small amounts of BT up to about x = 0.4, the coupling coefficient is slightly enhanced up to 0.64. At higher concentrations the coupling coefficient gradually decreases down to 0.33 for pure BT. This behavior is rather unusual because the presence of BT even in small amounts is expected to diminish the electromechanical factor k_p rather than to increase it.

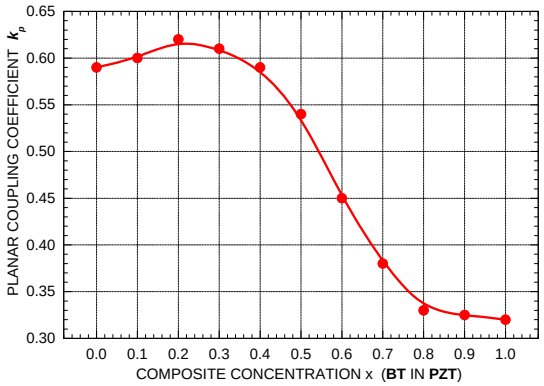

Fig. 8. The dependence of the electromechanical planar coupling factor on composition concentration x for sintered

A qualitative explanation for this behavior could be based on the fact that for smaller amounts of PZT particles into the BT matrix, the solving process of PZT is more complete as it take place at higher temperatures necessary to sinter BT and the new solid solutions formed are not within a morphotropic phase boundary and thus the poling cannot be entirely efficient. When the amounts of PZT and BT starts to equilibrate, the PZT phase become preponderant and k_p increases. A similar behavior was also recorded for the piezoelectric charge constant d_{33}, as shown in figure 9, where one can see that d_{33} increases from about 360 pC/N for x=0 up to 550 pC/N for x=0.4. At higher concentrations d_{33} constantly decreases down to $150 \cdot 10^{-3}$ m/V for pure PZT.

A similar behavior had the piezoelectric voltage constant g_{33} as well, as can be seen in Fig. 10.

All these results show that the sintering process between PZT and BT is a complex one. BT sinters and densifies at higher temperature and the presence of small amounts of PZT may react more intense with the BT particles at these higher temperatures forming a liquid phase while the PZT sinters and densifies at lower temperatures and the presence of BT in PZT at this temperatures does not produce well-formed solid solution.

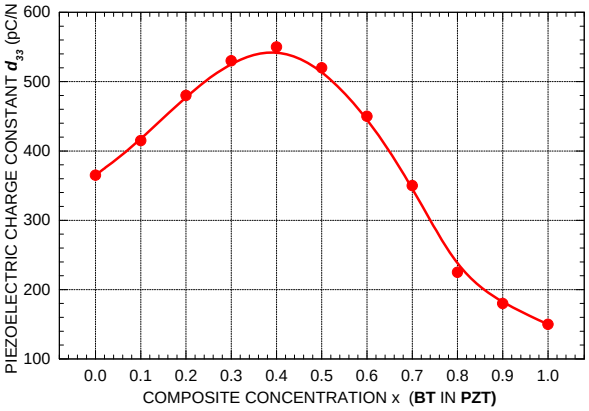

Fig. 9. The behaviour of piezoelectric charge constant, d_{33} as a function of the composition concentration, x, for sintered mixed PZT and BT samples

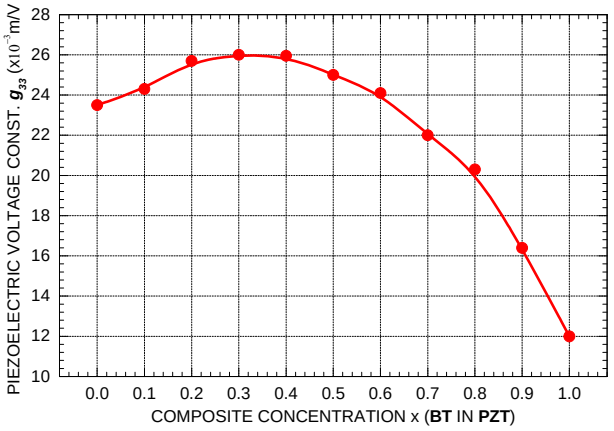

Fig. 10. The behavior of piezoelectric voltage constant, g_{33}, as a function of composition concentration x for sintered mixed PZT and BT samples

4. Conclusion

Sintered samples in the ferroic system (1-*x*)PZT·*x*BT with x = 0; 0.1; 0.2 … 0.9; 1 were investigated both structurally by X-ray diffraction and SEM microscopy and also from the piezoelectric point of view. The morphostructure of the samples is different, though X-ray patterns are similar for all compositions. This is due to the sintering process which depends on compositions taking place at different temperature for each composition. The dielectric properties showed a rather unusual behavior which was explained in terms of different grain size of the samples.

Remarkably, upon adding BT in PZT, a strong enhancement of the relative dielectric constant, ε_r, of roughly 4.7 times, is observed at a concentration of $x = 0.4$. The coupling coefficient, k_p, after a maximum at small BT concentrations, recovers at $x = 0.4$ the same value as in the pure PZT. Moreover, at this composition also the piezoelectric charge constant, d_{33} and the piezoelectric voltage constant g_{33} display clear maxima making the 0.6 PZT·0.4 BT compound a possible candidate for a large variety of applications.

Acknowledgments

This work was made in the frame of the NUCLEU Project-PN18-110201 and financed by the Ministry of Reaserch and Inovation. The authors acknowledge the financial support for making possible the dissemination of these results.

References

[1] H. Schmid, Ferroelectrics **162**(1), 317 (1994).
[2] N. Spaldin, M. Fiebig, Science **309**, 391 (2005).
[3] M. Fiebig, J. Phys. D: Appl. Phys. **38**, 123 (2005).
[4] W. Erenstein, N. Mathur, J. Scott, Nature **442**, 759 (2006).
[5] I. Dzyaloshinskii, Sov. Phys. JETP **10**, 628 (1959).
[6] M. Souni, S.P. Alpay, T. Shritharan, W. Prellier, U. V. Waghmare, J. Mat. Res. **22**(8), 2051 (2007).
[7] M. Taneef, H. Saleem, A. Habib, Synthetic Metals **223**, 101 (2017).
[8] J. Pintea, A. Dumitru, D. Patroi, G. Sbarcea, E. Manta, L. Leonat, J. Opt. Adv. M. **19**(11–12), 806 (2017).
[9] A. Pascu, E. M. Stanciu, D. Savastru, V. Geanta, C. Croitoru, J. Opt. Adv. M. **19**(1-2), 66 (2017).
[10] B. Pečar, H. Uršič, B. Malič, M. Možek, D. Vrtačnik, J. Opt. Adv. Mat. **19**(9-10), 617 (2017).
[11] M. Fiebig, T. Lottermoser, D. Frohlich, A. Goltsev, R. Pisarev, Nature **419**, 818 (2002).
[12] T. Lottemoser, T. Lonkai, U. Amann, D. Hohlwein, J. Ihringer, M. Fiebig, Nature **430**, 541 (2004).
[13] C. Nan, G. Liu, Y. Liu, H. Chen, Phys. Rev. Lett. **94**, 197203 (2005).
[14] J. Varghese, R. W. Whatmore, J. D. Holmes, Journal of Materials Chemistry C **1**(15), 2618 (2013).
[15] M. K. Lee, T. K. Nath, C. B. Eom, Appl. Phys. Lett. **77**(22), 3547 (2000).
[16] J. Ryn, A. Carazo, K. Uchino, H. Kini, Jpn. J. Appl. Phys. **40**, 4948 (2001).
[17] C. W. Nan, L. Liu, N. Cai, J. Zhai, Y. Ye, Y. H. Lin, Appl. Phys. Lett. **81**(20), 3831 (2002).
[18] N. Cai, C. Nan, J. Zhai, Y. Lin, Appl. Phys. Lett. **84**(18), 3516 (2004).
[19] B. J. Fang, W. W. Wang, J. N. Ding, X. Y. Zhao, H. Q. Xu, H. S. Luo, Advances in Applied Ceramics Structural, Functional and Bioceramics **112**(5), 257 (2013).
[20] J. Adam, T. Lehnert, G. Klein, R. M. McMeeking, Nanotechnology **25**(6), 065704 10 (2014).
[21] W. Choi, K. Choi, G. Yang, J. C. Kim, C. Yu, Polymer Testing **53**, 143 (2016).
[22] A. Moulson, J. Herbert, Electroceramics: Materials Properties and Application, Ed. John Wiley&Sons Ltd., Second Edition, (2003).
[23] Tae-Gon Lee, Ho-Jun Lee, Su-jin Park, Tae-Ho Lee, Dae-Hyeon Kim, Chang-Hyo Hong, Hai-Bo Xu, Chong Yun Kang, Sahn Nahm, J. Am. Cer. Soc. **100**(12), 5681 (2017).
[24] D. A. F. Benavides, A. I. G. Perez, A. M. B. Castro, M. T. A. Ayala, B. M. Murguia, J. M. Saldana, Materials **361**(11), 16 (2018); DOI:10.3390/MA11030361
[25] B. Jaffe, W. Cook, H. Jaffe, Piezoelectric ceramics, Acad. Press, London NY, ch. 4, 53 (1971).
[26] I. Fuji, K. Nakashima, N. Kumada, S. Wada, Journal of the Ceramic Society of Japan **120**(1), 30 (2012).
[27] Y. Mendez-Gonzales, A. Pelaiz-Barranco, J. D. S. Guerrab, A. Penton-Madrigal, P. Saint-Gregoire, Material Chemistry and Physics **208**, 103 (2018).
[28] G. Haertling, J. Am. Cer. Soc. **82**, 797 (1999).
[29] C. Miclea, C. Tanasoiu, L. Amarande, C. F. Miclea, Ferroelectrics **319**(1), 57 (2005).
[30] W. Chaisan, S. Ananta, T. Tunkariri, Current Appl.

Phys. **4**, 182 (2004).
[31] W. Chaisan, R. Yimnirun, S. Ananta, D. Cann, Mat. Lett. **59**, 3732 (2005).
[32] W. Chaisan, R. Yimnirun, S. Ananta, Ceramics International **35**, 121 (2009).
[33] R. Yimnirum, Ferroelectrics **311**, 9 (2006).
[34] R. Yimnirum, S. Ananta, S. Chamunglap, Mat. Chem. Phys. **102**, 165 (2007).
[35] W. Chaisan, R. Yimnirun, S. Ananta, D. Cann, Mat. Chem. Phys. **104**, 113 (2007).
[36] L. Eyrand, B. Guiffard, L. Lebrun, D. Guyomar, Ferroelectrics **330**, 51 (2006).
[37] H. Li, C. Tian, Z. D. Deng, Appl. Phys. Rev. **1**(4), 041301 (2014).
[38] R. German, Sintering Theory and Practice, Ed. John Willey&Sons, NY, (1996).
[39] M. N. Rahaman, Ceramic Processing and Sintering – Second Edition, Taylor & Francis eBooks, (2003).
[40] D. Zhang, G. Weng, S. Gong, D. Zhou, Mat. Sci. Eng. B **99**, 88 (2003).
[41] R. Roseman, N. Mukherjee, J. Electroceramics, **10**, 117 (2003).
[42] A. Bell, A. Moulson, L. Cross, Ferroelectrics **54**, 147 (1984).
[43] K. Gachigi, U. Kumar, J. Dougherty, IEEE Sym. Appl. of Ferroelectrics **47**, 492 (1992).
[44] W. Luan, L. Gao, J. Guo, Ceramic Int. **25**, 727 (1999).
[45] G. Artl, H. Penses, Ferroelectrics **48**, 213 (1983).
[46] B. Stojanovic, C. Foschini, M. Zagheti, F. Veira, K. Peron, M. Cilense, J. Varela, J. Mat. Process. Techn. **143-144**, 802 (2003).

*Corresponding author: cmic@infim.ro